Effect of Lubricant Rheology on Friction in Coated Elastohydrodynamic Lubricated Contacts

W. Habchi[1,2,*,#] and S. Bair [2]

[1]Lebanese American University, Department of Industrial and Mechanical Engineering, Byblos, Lebanon

[2]G.W. Woodruff School of Mech. Eng., Center for High Pressure Rheology, Georgia Institute of Technology, Atlanta, GA 30332-0405

*Corresponding author: wassim.habchi@lau.edu.lb , Phone: +961-9-547262 , Fax: +961-9-547256

#At the time this work was done, the first author was holding a visiting scholar position at Georgia Institute of Technology

Abstract

This work investigates the effect of lubricant rheology on friction in coated elastohydrodynamic contacts. Two lubricants with relatively different properties are selected and two coating configurations are considered. The first coating type consists of a soft material with a low thermal inertia while the second is a hard material with a high thermal inertia. The former is known to decrease friction while the latter increases it compared to uncoated contacts. The original expectation was that the lubricant with higher *P-T* dependence of viscosity would exhibit higher relative friction deviation from the uncoated case. It turned out that this is only true in the linear and thermo-viscous friction regimes at low and high slide-to-roll ratios respectively.

Keywords: Elastohydrodynamic Lubrication; Surface Coatings; Lubricant Rheology; Friction;

1. Introduction

Surface coatings have for some time been considered for improving the tribological performance of contacting machine elements with relative motion. First, the technology was used in dry contacts but over the last few decades, its use has extended to lubricated contacts. In particular, surface coatings are earning growing attention with elastohydrodynamic lubricated (EHL) contacts. This is because it was found, from the earliest studies on the topic, that coatings may have a significant influence on the performance of machine elements such as gears, bearings and cam-followers which operate under the EHL regime. For a long time, the focus was on the mechanical and surface finishing characteristics of coatings which were chosen to reduce wear and fatigue of corresponding components. Surface finishing also has a significant effect on friction as it was pointed out for instance by Masjedi and Khonsari [1] in their simulations of rough EHL line contacts validated by experiments or also in the numerical simulations of Xu and Sadeghi [2] or the experiments of Björling et al. [3] for circular contacts.

To the authors' knowledge, one of the first works to investigate the effect of thermo-mechanical properties of surface coatings on EHL friction is that of Bogdanski [4]. More recently, this effect has started to gain more attention, with experimental works such as that of Evans et al. [5] or Kalin et al. [6], who reported reduced friction in Diamond-Like-Carbon (DLC) coated EHL contacts compared to equivalent uncoated contacts. At first, the friction reduction was thought to be a consequence of boundary slip. However, Björling et al. [7] later reported

friction reductions in DLC coated EHL contacts under full film regime with a combined root-mean-square roughness of the coating surfaces of the order of 155-355nm. Under such conditions, boundary slip is highly unlikely to occur which led the authors to assume that the observed friction reductions might rather be, at least in part, a thermal phenomenon. This hypothesis was later verified in [8], where the experimental results were validated against numerical simulations using the finite element full-system approach [9] which does not include boundary slip. The thermal origins of the observed friction reductions were later investigated in detail by Habchi [10]. In the latter work, it was found that a low thermal inertia coating (compared to the substrate) like DLC, acts as an insulator, reducing heat removal from the contact towards peripheral regions. This leads to increased temperatures inside the film, resulting in reduced lubricant viscosity in that same region and as a result, reduced friction. Similar findings were later reported in experiments of DLC coated contacts, supported by numerical confirmation by Bobach et al. [11] or also Bobzin et al. [12] for automotive applications. Beilicke et al. [13] also provided similar numerical findings for DLC coated contacts in helical gear pairs under transient thermal EHL operation. In [10], it was also shown that friction may also be increased, if needed by the application at hand, by using a high thermal inertia coating which has the opposite effect.

In a later work, Habchi [14] showed that not only the thermal properties of surface coatings affect friction in EHL contacts, but also mechanical properties may have a significant effect, through a different mechanism. In fact, it was shown that a soft coating (compared to the substrate) can lead to reduced friction compared to the uncoated case because of the lower contact pressures that are involved. These lead to reduced lubricant viscosity over the contact domain and, as a consequence, reduced friction. Hard coatings have the exact opposite effect and lead to increased friction. Also, the mechanical properties of coatings were shown to influence friction irrespective of slide-to-roll ratio (*SRR*) whereas thermal properties only had a significant effect beyond a threshold *SRR* where heat generation became pronounced. This is not surprising, as friction variations in the latter case are the result of a purely thermal phenomenon whereas in the former case, they are the result of a pressure variation which is independent of contact kinematics. It only depends on the employed solid material properties for the coating and substrate. Obviously, the combination of soft coating material with low thermal inertia leads to the greatest friction decrease whereas the combination of hard material with high thermal inertia leads to the greatest friction increase. A very important aspect of these friction variations lies in the fact that film thicknesses in the corresponding contacts were observed to be very little affected. Thus, friction may be controlled by a suitable choice of surface coating based on its thermo-mechanical properties without significant impact on the corresponding component life. In [14], the effects of thermo-mechanical properties of a coating on friction were shown to increase with its thickness. However, for the effect of coating thermal properties on friction, a limiting coating thickness value was found beyond which the thermal boundary layer of the contacting solids would entirely fall within the coating. As such, any further increase in coating thickness would have no effect on contact temperature and, as a consequence, no effect on

friction. A limiting value was not found for the effect of coating mechanical properties on friction, as for this to happen, the coating thickness should be great enough for the coating itself to occupy a half-space such that the substrate properties would no longer affect contact pressure. Obviously, in practice this is never the case, otherwise the added surface layer no longer qualifies as a coating. The increase in friction deviation with coating thickness with respect to the uncoated case was experimentally validated by Björling et al. [15].

The current work comes as a logical continuation of the aforementioned works on the effects of coatings and their properties on EHL friction. In all of these, only one well characterized lubricant was employed in the analysis. In the current work, two well characterized lubricants, a mineral oil (Shell T9) and a polyalphaolefin (PAO4) with relatively different rheological properties are considered. The general idea is to investigate and understand the effects of lubricant rheological differences on the frictional response of coated EHL contacts. This would allow a better informed lubricant selection for such applications.

2. Lubricant Selection and Properties

In order to understand the effects of lubricant rheological differences on friction in coated EHL contacts, two lubricants with relatively different rheological properties are considered: a mineral oil (Shell T9) and a polyalphaolefin (PAO4). The viscosity of the former exhibits a relatively high *P*-*T*-dependence while that of the latter is relatively low. The two fluids are well characterized and their rheological behavior well identified which makes them perfect candidates for the current study. It should be mentioned that, although the description of PAO4 (4centiStoke at 100°C) is generic, there is little variation in the *P*-*T*-dependence among samples from various commercial suppliers.

Next, the different rheological models employed in describing the dependence of the two lubricants transport and thermal properties on pressure, temperature and shear stress are described. The values of the different parameters of each model for the two considered lubricants are summarized in Table 1. In the following, subscripts *0* and *R* indicate, respectively, ambient pressure and temperature state ($p_0 = 0$ and $T_0 = 30^o\mathrm{C}$) and a reference state ($p_R = 0$ and $T_R = 25^o\mathrm{C}$). Density variations with pressure and temperature are described by the Murnaghan [16] equation of state:

$$\rho = \frac{\rho_R}{1 + a_V\left(T - T_R\right)} \times \left(1 + \frac{K_0'}{K_0}\, p\right)^{\frac{1}{K_0'}} \quad \text{with} \quad K_0 = K_{00}\exp\left(-\beta_K T\right) \tag{1}$$

The low-shear *P*-*T*-dependence of viscosity is described by a thermodynamic scaling function [17] [18] as follows:

$$\mu = \mu_\infty \exp\left(\frac{B_F \varphi_\infty}{\varphi - \varphi_\infty}\right) \quad \text{with} \quad \varphi = \left(\frac{T}{T_R}\right)\left(\frac{V}{V_R}\right)^g \tag{2}$$

Where $V/V_R = \rho_R/\rho$ is described by the Murnaghan equation of state as provided in equation (1). For T9, the density and viscosity data as well as values of the different parameters in equations (1) and (2) can be found in [19], and for PAO4 the viscosity data used in generating these parameters can be found in [20] and [21]. The relative volume data for PAO4 was obtained through measurements with a metal bellows piezometer, carried out at the Center for High Pressure Rheology, at the Georgia Institute of Technology. Figure 1 shows the viscosity dependence on pressure for the two considered lubricants as described by the combination of the Murnaghan equation of state in equation (1) and the thermodynamic scaling function of equation (2) at three different temperatures (30, 70 and 100^{o}C). The stronger pressure and temperature dependence of T9 can be readily seen in Figure 1. Though at ambient pressure both fluids have comparable pressure and temperature dependence, at high pressure, the higher sensitivity of T9 becomes apparent.

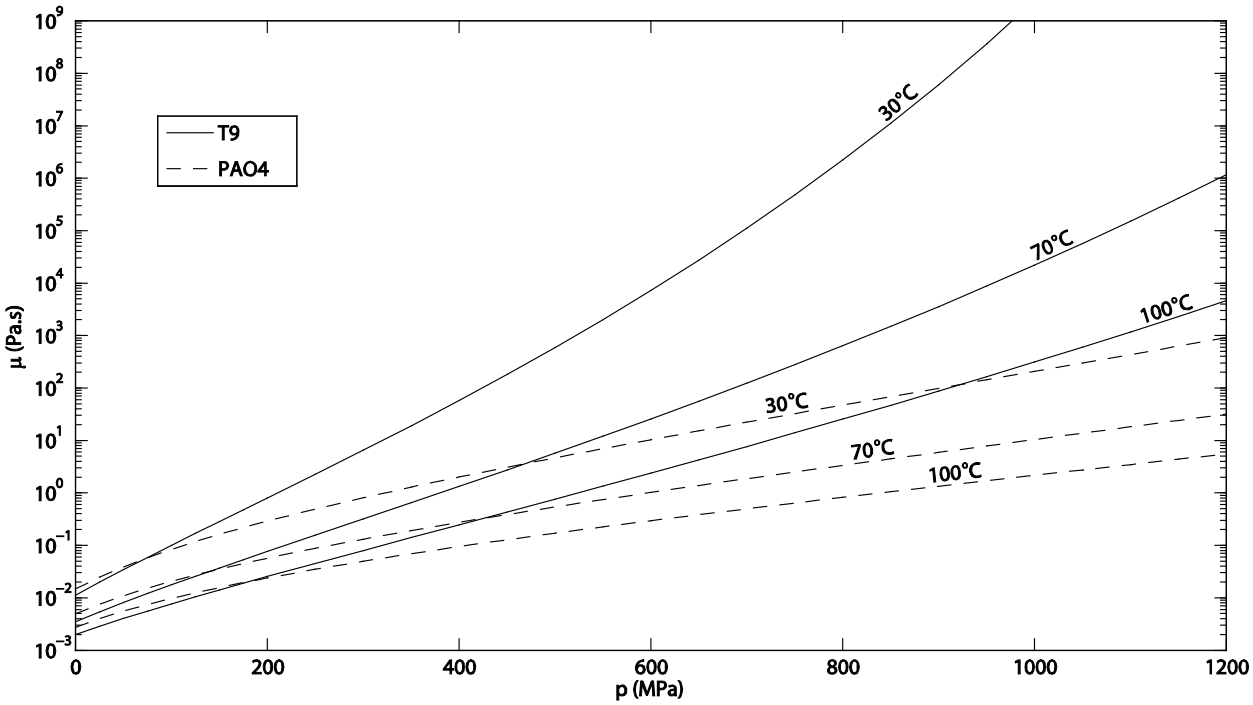

Figure 1: Low shear viscosity dependence on pressure for T9 and PAO4 as described by the thermodynamic scaling function

For the shear dependence of viscosity, the single-Newtonian modified Carreau-Yasuda model [22] is used to describe the dependence of the generalized viscosity η on shear stress τ:

$$\eta = \frac{\mu}{\left[1+\left(\frac{\tau}{G}\right)^a\right]^{\frac{\frac{1}{n}-1}{a}}} \tag{3}$$

For T9, the viscosity data as well as the values of the different parameters in equation (3) can be found in [19], and for PAO4 the viscosity data used in generating these parameters can be found in [23]. Figure 2 shows the shear dependence of viscosity for the two considered lubricants as described by equation (3). It is clear that T9 exhibits a stronger shear-thinning behavior than PAO4 as evidenced by a faster viscosity decrease with shear stress. Also note that shear-thinning effects appear at lower shear stresses for T9 because of its lower effective shear modulus G.

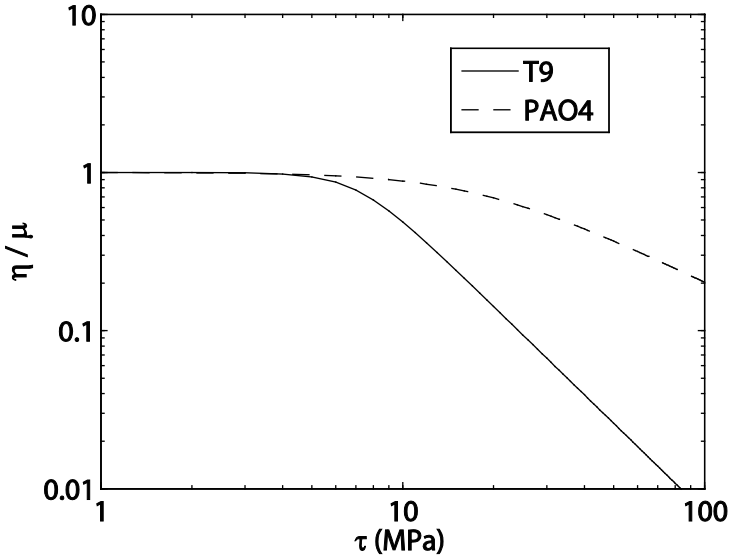

Figure 2: Shear dependence of viscosity for T9 and PAO4 as described by the single-Newtonian modified Carreau-Yasuda model

The limiting-shear-stress τ_L is assumed to vary linearly with pressure as suggested in [24]:

$$\tau_L = \Lambda\, p \tag{4}$$

The values of the limiting stress-pressure coefficient Λ are deduced from EHL experimental traction curves obtained under near isothermal operating conditions. For T9, these curves can be found in [19] and for PAO4 they can be found in [25]. Here, Λ is assumed to be independent of temperature and while this is approximately true (Λ should decrease slowly with temperature), it must be recognized that this assumption will have an effect on conclusions drawn from the simulations.

Finally, in [19] Habchi et al. pointed out the importance of accounting for the *P-T*-dependence of the lubricant thermal properties for an accurate prediction of friction in the thermo-viscous regime [26]. In fact, it was shown that failing to account for the variations in thermal properties of the lubricant within EHL conjunctions leads to an under-estimation of friction in the thermo-viscous regime. To model this dependence, a scaling rule was suggested in [19]. Thermal conductivity k is given by:

$$k = B_k + C_k \kappa^{-s} \qquad \text{with} \qquad \kappa = \left(\frac{V}{V_R}\right)\left[1 + A\left(\frac{T}{T_R}\right)\left(\frac{V}{V_R}\right)^3\right] \tag{5}$$

The expression for volumetric heat capacity $C = \rho c$ reads:

$$C = C' + m\chi \qquad \text{with} \qquad \chi = \left(\frac{T}{T_R}\right)\left(\frac{V}{V_R}\right)^{-4} \tag{6}$$

For T9, the thermal conductivity and volumetric heat capacity data, as well as the values of the different parameters in equations (5) and (6), can be found in [19]. For PAO4, the *P*-*T*-dependence of thermal properties is not known. It was assumed that these will exhibit variations similar to those of T9 while adjusting the parameters B_k and C' by shifting them to match the ambient values for PAO4, which are known.

Model	Parameter	T9	PAO4
Murnaghan EOS Equation (1)	$\rho_R\,(\mathrm{kg/m^3})$	875	810
	$a_V\,(\mathrm{K^{-1}})$	7.734×10^{-4}	8.475×10^{-4}
	K_0'	10.545	11.600
	$K_{00}\,(\mathrm{GPa})$	9.234	13.949
	$\beta_K\,(\mathrm{K^{-1}})$	6.090×10^{-3}	7.766×10^{-3}
Thermodynamic scaling function Equation (2)	$\mu_\infty\,(\mathrm{Pa\cdot s})$	1.489×10^{-4}	1.311×10^{-4}
	B_F	12.898	16.484
	φ_∞	0.26844	0.24541
	g	5.0348	3.5602
Carreau-Yasuda Equation (3)	$G\,(\mathrm{MPa})$	7	18
	a	5	2
	n	0.35	0.52
Limiting-Shear-Stress Equation (4)	Λ	0.083	0.06
k -scaling Equation (5)	$B_k\,(\mathrm{W/m\cdot K})$	0.053	0.080
	$C_k\,(\mathrm{W/m\cdot K})$	0.026	0.026
	A	-0.101	-0.101
	s	7.6	7.6
C -scaling Equation (6)	$C'\,(\mathrm{J/m^3\cdot K})$	1.17×10^6	1.35×10^6
	$m\,(\mathrm{J/m^3\cdot K})$	0.39×10^6	0.39×10^6

Table 1: Parameters for the models describing the rheological behavior of the two employed lubricants (T9 and PAO4)

Though rather complex, the above detailed description of lubricant constitutive behavior, based on measured laboratory data of the considered properties, is essential for an accurate and realistic quantitative prediction of friction in EHL contacts as discussed in [27].

3. Numerical Model Description

The numerical model employed in this work is described in detail in [28]. Here, only the essential features are briefly recalled for completeness. The model is based on a finite element discretization of the thermal elastohydrodynamic lubrication (TEHL) problem equations. These are: the generalized Reynolds, linear elasticity and load balance equations for the EHL part and the energy equation applied to the solids (substrates and coatings) and lubricant film for the thermal part. The unknowns / field variables for the former are the pressure and film thickness distributions over the contact domain while for the latter the field variable corresponds to the temperature distribution within the solids and lubricant film. The generalized Reynolds equation accounts for lubricant viscosity and density variations across the lubricant film thickness as a consequence of shear-thinning as well as temperature variations. Starting from a properly selected initial guess for pressure, film thickness and temperature, first the EHL part is solved in a full-system approach for a given temperature distribution. This gives rise to updated pressure and film thickness profiles. Then, the thermal part is solved for given pressure and film thickness distributions as obtained from the EHL part. Thus, a new temperature profile within the solids and lubricant film is obtained. This procedure of consecutive resolution of the EHL and thermal parts is repeated until converged pressure, film thickness and temperature distributions are attained.

4. Results and Discussion

In this section, the effect of lubricant rheological differences (T9 vs. PAO4) on friction in EHL contacts is discussed. Smooth circular contacts subject to a fixed external applied load F are considered under steady-state considerations. A fully-flooded regime is assumed and the surfaces are considered to be fully separated by the lubricant film. The geometry of such contacts can be reduced to an equivalent contact between a ball of radius R and a flat plane as shown in Figure 3. Rolling-sliding conditions are assumed with unidirectional surface velocities u_b and u_p in the entrainment direction x.

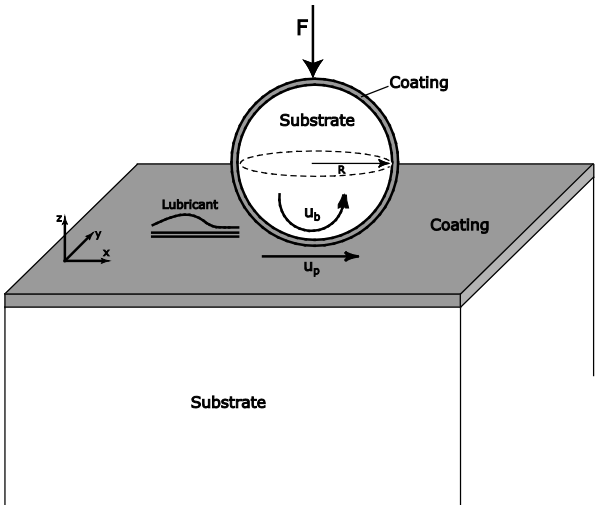

Figure 3: Geometry of the coated TEHD circular contact

Both surfaces are assumed to be either uncoated or coated with the same coating material and thickness. Coatings are assumed to be perfectly bonded to the substrates. The material of the substrates is taken to be steel. Two types of coating materials are considered. The first has a Young's modulus of elasticity E and thermal inertia $I = \sqrt{kC}$ that are smaller than those of the substrate and it is referred as "Soft + Low I" while for the second they are higher and it is called "Hard + High I". These are the same coating types as employed in [14]. They are not intended to represent any specific existing materials but were rather selected to cover a range of values of thermal inertia and rigidity. The former is a relevant property when it comes to heat removal from the contact, while the latter governs the central contact pressure. Both have a significant influence on friction as discussed earlier. The mechanical and thermal properties of the substrate and different coating materials as well as the operating conditions are summarized in Table 2. Four different external applied loads F = 5, 10, 25 and 100N are considered with corresponding Hertzian contact pressures p_h = 0.43, 0.54, 0.74 and 1.17 GPa respectively. These Hertzian contact pressure values are the ones obtained for an uncoated contact. Obviously, in a coated contact the values will be altered depending on the type of coating as discussed earlier. A soft coating would lead to reduced Hertzian contact pressure while a hard coating would increase it. The combinations of soft coating material with low thermal inertia or hard material with high thermal inertia were chosen so that the coating would have the greatest possible impact on friction. The first combination reduces friction while the second increases it compared to an equivalent uncoated contact as discussed in [14]. Two different mean entrainment speeds u_m = 0.2 and 1.0 m/s are employed. Low speed is used in combination with low loads (5 and 10N) to avoid reaching limiting-shear-stress under these conditions. This is because when reached, it dominates the frictional response of the contact and smears out other effects as will be discussed later. For the higher loads (25 and 100N), limiting-shear-stress is reached anyway (even at low speeds), so the higher speed of 1m/s is employed to ensure sufficient heat generation for the thermo-viscous friction regime to be reached as discussed later. This way, all possible friction regimes would be covered and a comprehensive analysis would be offered. Three different coating thicknesses t_c = 20, 40 and 80 μm and a range of slide-to-roll ratios $0.0 \le SRR \le 0.5$ are considered.

<table>
<tr><td rowspan="2">Operating conditions</td><td colspan="3">Solid material properties</td></tr>
<tr><td>Substrate</td><td colspan="2">Coatings</td></tr>
<tr><td rowspan="6">T_0=30ºC
u_m=0.2; 1m/s
SRR=0.0-0.5
F=5; 10; 25; 100N
p_h=0.43; 0.54; 0.74; 1.17GPa
R=12.7mm
t_c=20; 40; 80μm</td><td rowspan="6">E_s=210GPa
υ_s=0.3
ρ_s=7850kg/m^3
k_s=46W/m.K
c_s=470J/kg.K</td><td>Mechanical properties</td><td colspan="2">Thermal properties</td></tr>
<tr><td rowspan="5">$E_c = \begin{cases} 105\,\text{GPa (Soft)} \\ 420\,\text{GPa (Hard)} \end{cases}$
υ_c=0.3</td><td>Low I</td><td>High I</td></tr>
<tr><td rowspan="4">ρ_c=3500kg/m^3
k_c=5W/m.K
c_c=200J/kg.K</td><td rowspan="4">ρ_c=10000kg/m^3
k_c=90W/m.K
c_c=1000J/kg.K</td></tr>
<tr></tr>
<tr></tr>
<tr></tr>
</table>

Table 2: Operating conditions and solid material properties

In the following, friction coefficients *f* are evaluated by an integration of shear stresses in the *x*-direction τ_{zx} within the mid-layer of the lubricant film ($z = h/2$), over the contact domain, Ω_c , as follows:

$$f = \frac{\int_{\Omega_c} \tau_{zx}\big|_{z=h/2}\, d\Omega}{F} \tag{7}$$

In order to assess the impact of surface coatings on friction, a parameter, ξ, is defined to quantify relative friction deviations in a coated contact with respect to the equivalent uncoated case over the considered range of *SRR*, as follows:

$$\xi = \frac{\int_{0.0}^{0.5} \left(f_{coated} - f_{uncoated} \right) dSRR}{\int_{0.0}^{0.5} f_{uncoated}\, dSRR} \tag{8}$$

Obviously, a positive value of ξ implies an increase in friction which would be obtained in the current work with a "Hard + High I" coating while a negative value implies a friction decrease which would be obtained if a "Soft + Low I" coating is employed.

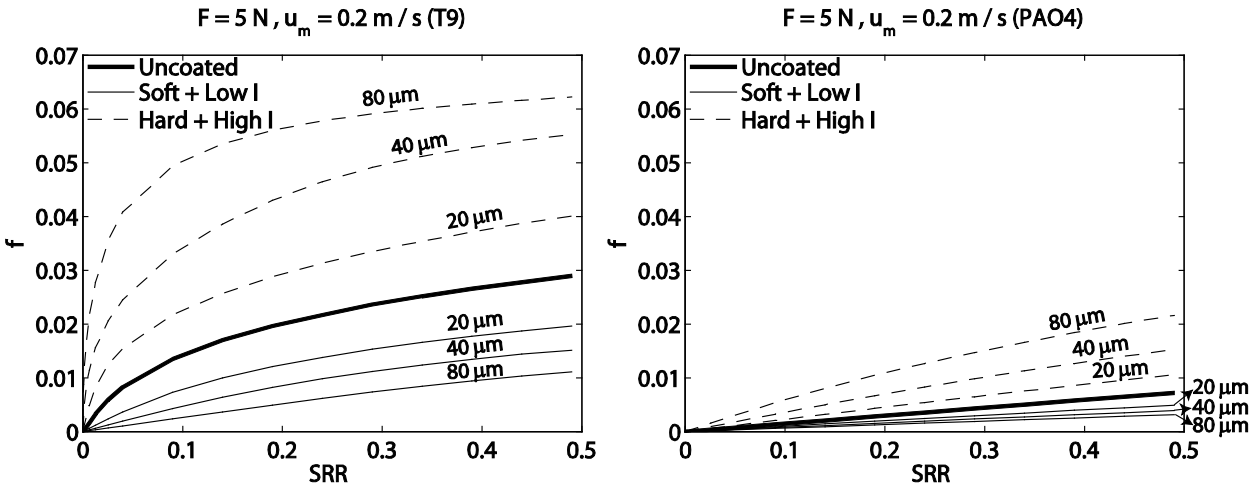

Figure 4: Friction curves for the "Uncoated", "Soft + Low I" and "Hard + High I" cases for F = 5 N (p_h = 0.43 GPa) and u_m = 0.2 m/s for three different coating thicknesses (t_c = 20, 40 and 80µm). Left: T9, right: PAO4.

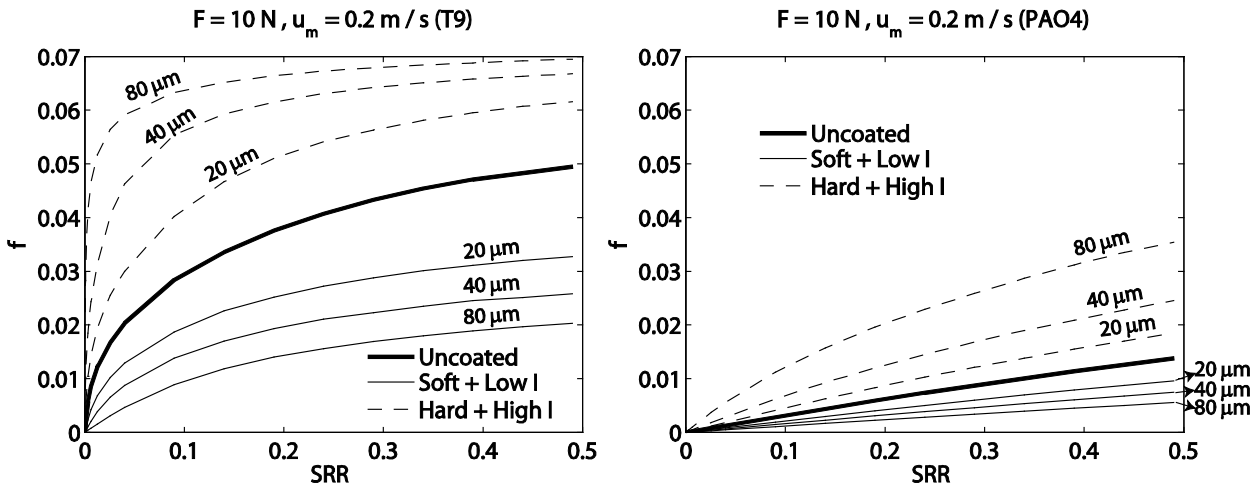

Figure 5: Friction curves for the "Uncoated", "Soft + Low I" and "Hard + High I" cases for F = 10 N (p_h = 0.54 GPa) and u_m = 0.2 m/s for three different coating thicknesses (t_c = 20, 40 and 80µm). Left: T9, right: PAO4.

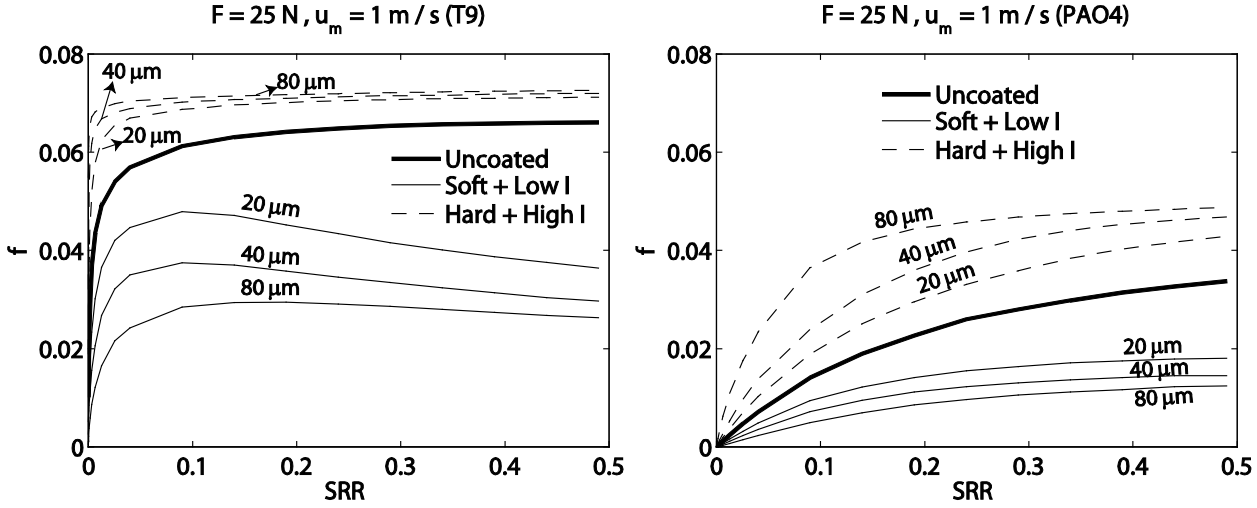

Figure 6: Friction curves for the "Uncoated", "Soft + Low I" and "Hard + High I" cases for F = 25 N (p_h = 0.74 GPa) and u_m = 1 m/s for three different coating thicknesses (t_c = 20, 40 and 80µm). Left: T9, right: PAO4.

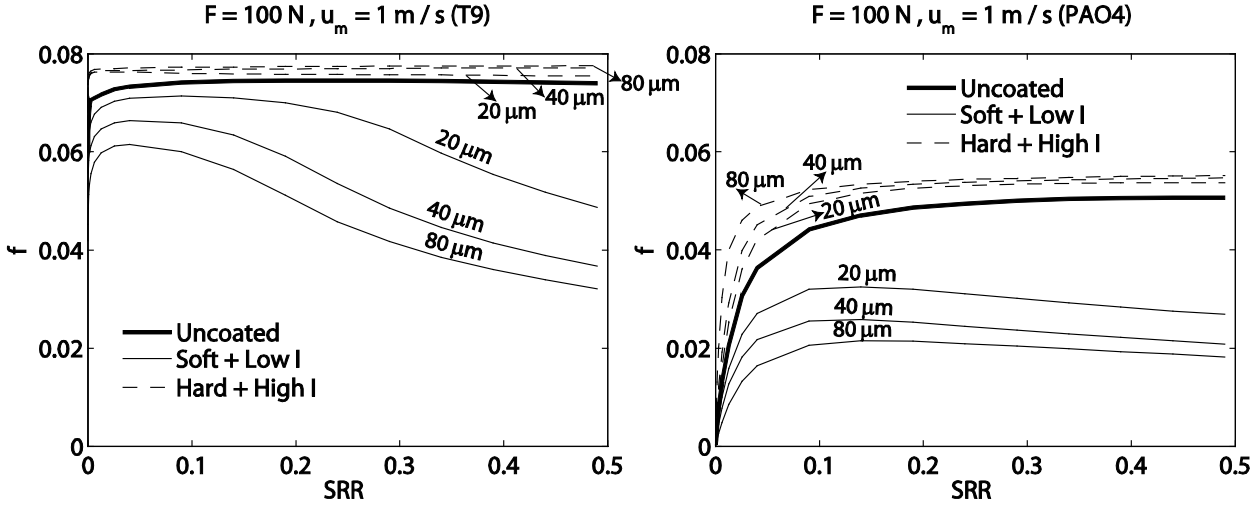

Figure 7: Friction curves for the "Uncoated", "Soft + Low I" and "Hard + High I" cases for F = 100 N (p_h = 1.17 GPa) and u_m = 1 m/s for three different coating thicknesses (t_c = 20, 40 and 80µm). Left: T9, right: PAO4.

Figures 4, 5, 6 and 7 show the friction curves for the four external applied loads F = 5, 10, 25 and 100N respectively under all coating configurations and thicknesses for the two lubricants selected for this work. The uncoated case is shown in all figures as a reference for comparison. The value of the relative friction deviation from the uncoated case parameter ξ for each friction curve is reported in Table 3 along with the corresponding maximum value of the Weissenberg *Wi* [29] and limiting-shear-stress *Li* [26] dimensionless numbers. These are evaluated at the contact center within the mid-layer of the lubricant film and are defined as follows:

$$Wi = \frac{\tau}{G} \quad \text{and} \quad Li = \frac{\tau_u}{\tau_L} \quad \text{with} \quad \tau = \sqrt{\tau_{zx}^2 + \tau_{zy}^2} \tag{9}$$

Where τ_u is the unbounded value of τ (not limited by τ_L). It is important at this point to mention the relevance of the *Wi* and *Li* dimensionless numbers when it comes to defining friction regimes [26]. A value of $Wi > 1$ indicates the onset of shear-thinning since the shear stress within the lubricant film would have exceeded the Newtonian limit G of the lubricant. *Wi* is used as an indicator for the transition from the linear to nonlinear friction regime. A value of $Wi < 1$ indicates that a linear regime prevails in which shear-thinning is absent and friction increases linearly with *SRR* since frictional response is governed by the Newtonian / low shear viscosity of the lubricant (or the elastic creep of the contacting solids at high pressures and very low *SRR* [30]). When the value of *Wi* exceeds unity, frictional response departs from linear behavior and the slope of the friction curve decreases with *SRR* revealing the non-linear friction regime. The limiting-shear-stress number *Li* on the other hand is an indicator of whether or not limiting-shear-stress is reached within the contact. A value of $Li < 1$ indicates that it hasn't been reached since it implies that $\tau < \tau_L$. A value of $Li > 1$ indicates that limiting-shear-stress is reached within the lubricant film and the higher the value of *Li*, the larger the area of the contact over which limiting-shear-stress is reached. The values of *Wi* and *Li* reported in Table 3 correspond to the maximum values for a given friction curve obtained at a given *SRR*, which is not necessarily the same for all considered cases. It corresponds to the highest considered value in this work (*SRR*=0.5) for all cases except for the 25 and 100N cases for T9 and the 100N case for PAO4, where for these cases, maximum values of *Wi* and *Li* are in the vicinity of $SRR \approx 0.15$.

Coating Type	Operating Conditions	t_c (μm)	T9			PAO4		
			ξ (%)	*Wi*	*Li*	ξ (%)	*Wi*	*Li*
Soft + Low I	F = 5 N, u_m = 0.2 m/s	20	-36.81	1.99	0.44	-31.80	0.19	0.15
		40	-54.73	1.44	0.35	-45.70	0.13	0.11
		80	-70.06	0.99	0.28	-56.35	0.08	0.08
	F = 10 N, u_m = 0.2 m/s	20	-33.91	4.13	0.70	-31.24	0.51	0.31
		40	-49.29	2.91	0.54	-47.14	0.36	0.24
		80	-62.68	1.95	0.42	-60.96	0.21	0.16
	F = 25 N, u_m = 1.0 m/s	20	-33.32	8.14	0.99	-41.29	0.99	0.43
		40	-47.04	6.04	0.79	-53.38	0.76	0.35
		80	-56.78	4.26	0.63	-62.95	0.59	0.31
	F = 100 N	20	-13.69	13.34	1.22	-37.38	3.05	0.81

	u_m = 1.0 m/s	40	-28.63	12.74	1.05	-50.70	2.31	0.64
		80	-36.98	11.28	0.96	-58.51	1.87	0.57
Hard + High I	F = 5 N u_m = 0.2 m/s	20	+46.02	4.29	0.76	+48.88	0.45	0.29
		40	+114.07	6.58	1.26	+123.43	0.82	0.44
		80	+170.88	7.77	2.04	+233.77	1.47	0.68
	F = 10 N u_m = 0.2 m/s	20	+32.15	6.93	1.44	+37.70	0.99	0.51
		40	+57.83	7.68	1.82	+90.97	1.42	0.66
		80	+73.39	9.35	2.48	+196.37	2.62	1.07
	F = 25 N u_m = 1.0 m/s	20	+10.30	9.35	2.01	+29.25	2.62	1.08
		40	+12.31	9.84	2.13	+51.66	2.77	1.17
		80	+13.71	11.83	2.42	+78.69	3.32	1.45
	F = 100 N u_m = 1.0 m/s	20	+2.23	14.57	2.22	+8.24	4.09	1.79
		40	+3.72	14.87	2.37	+10.90	4.18	1.91
		80	+4.33	16.17	2.44	+13.83	4.55	2.12

Table 3: Friction deviation in coated EHL contacts compared to the equivalent uncoated case

Looking at Figures 4-7, it is clear that a "Soft + Low I" coating leads to decreased friction compared to the uncoated case whereas a "Hard + High I" coating increases friction. Also one can clearly see that friction variations with respect to the uncoated case increase with coating thickness. This is in line with the observations made in [14] where the underlying mechanisms behind these observations are thoroughly discussed. Also note that for PAO4, friction coefficients are always lower than T9 for the same operating conditions. This is not surprising though, since the former has a relatively lower viscosity (as can be seen in Figure 1) and limiting-shear-stress coefficient Λ than the latter.

Next, the effect of lubricant rheological differences on relative friction variations in coated contacts compared to the uncoated case is discussed. One would expect that T9, which has a higher *P-T* dependence of viscosity than PAO4 would have higher ξ values under all conditions. This is because the origins of friction variations in coated compared to uncoated contacts are related to pressure and temperature differences between the two cases. As explained earlier and detailed in [14], a soft coating leads to decreased contact pressures leading to reduced lubricant viscosity and as a consequence lower friction. On the other hand, a low thermal inertia coating acts as a thermal insulator, reducing heat removal from the lubricant film. This leads to increased film temperature and as a consequence reduced lubricant viscosity and friction. Opposite effects would be obtained with a hard and / or high thermal inertia coating. A close look at the results of Table 3 reveals that the expectation that the values of ξ be higher for T9 than PAO4 under all conditions is not met, at least not under all conditions. This reveals the complexity of EHL friction and the variety of underlying physics and regimes as shall be discussed next. In fact, in order to understand why the actual outcome differs from expectations (at least in some cases), the results of Table 3 need to be examined in detail.

Starting with the friction reducing coating configuration "Soft + Low I", for the 5 and 10N cases, the outcome is as expected and T9 exhibits a stronger relative friction decrease than PAO4. Note that for both lubricants and both loads, limiting-shear-stress is not reached ($Li < 1$). For PAO4, even shear-thinning and the non-linear friction regime is not reached ($Wi < 1$) as also

evidenced by the corresponding linear friction curves in Figure 4 (right). However, note that for the 10N case, the values of ξ for the two lubricants are less disparate than for the 5N case. This is because in the former case, for T9, the non-linear regime is reached ($Wi > 1$) while for PAO4 it isn't. In the non-linear regime, the extent of relative friction reduction with respect to the uncoated case is mitigated by shear-thinning compared to the linear regime. Shear-thinning reduces the temperature dependence in a rate controlled process [31]. The effect of reduced ξ values in the non-linear compared to the linear friction regime can be observed for PAO4 taken separately. In fact, note how for PAO4, ξ values increase (in absolute value) with load as long as the non-linear regime is not reached (for the 5, 10 and 25N cases). However, as soon as the non-linear regime is reached (100N case), the tendency is inverted. This inverted tendency is observed for T9 from the lowest considered load here (F=5N) since even in that case, the non-linear friction regime is already reached. The mitigation effect continues at higher loads and even reverses the tendency at 25N where values of ξ are now higher (in absolute value) for PAO4 than for T9. For both lubricants, the limiting-shear-stress is still not reached in this case. However, for T9 the non-linear regime is penetrated deeply ($Wi \gg 1$) whereas for PAO4 the entire friction curves still fall in the linear regime. For T9, the thermo-viscous regime is even reached, as indicated by the shape of the corresponding friction curves in Figure 6 (left), which exhibit a friction decrease with sliding speed at high *SRR*. The effect of stronger relative friction reduction for PAO4 compared to T9 is further amplified for the 100N case. Although the non-linear friction regime is now reached for PAO4, for T9 much more of the contact is in this regime with increasingly higher *Wi* values. Add to this, in the T9 case, limiting-shear-stress is now reached ($Li > 1$). The latter does more than reducing the relative friction deviation; it cuts it off. In fact, shear stress in this regime is bounded by a limiting value which only increases linearly with pressure, compared to viscosity variations with pressure which govern frictional response in the linear regime and which are far stronger than linear.

In the thermo-viscous regime (at high *SRR*), where friction decreases with increasing sliding speeds due to thermo-viscous effects, T9 exhibits a more pronounced friction decrease than PAO4 as evidenced by the steeper slopes of the corresponding friction curves in Figure 6. This is because in the thermo-viscous regime, limiting-shear-stress is no longer reached [26] and the frictional response of the contact goes back to being dominated by the thermo-viscous response of the lubricant. Since, T9 has a stronger *P-T* dependence than PAO4, it exhibits a steeper friction decrease. Note that for PAO4, the thermo-viscous regime is reached without going through the "Plateau" or limiting-shear-stress regime in this case. The fact that the non-linear regime is reached at lower loads for T9 compared to PAO4 is not surprising since the former exhibits a stronger shear-thinning response as evidenced by Figure 2. Also, the fact that limiting-shear-stress is reached at lower loads for T9, even though it has a lower limiting-shear-stress coefficient Λ, is not surprising. This is because T9 has a much higher viscosity than PAO4 at pressures exceeding 200MPa, as evidenced by Figure 1.

Moving to the friction increasing coating configuration “Hard + High I”, it is clear that the outcome does not meet the expectations for all considered test cases. In fact, PAO4 exhibits a stronger relative friction increase compared to T9 even for the lowest considered load of 5N. This is because, even for this case, both the non-linear friction regime and limiting-shear stress are reached for T9 whereas for PAO4 they are almost not. In fact, for PAO4, for a coating thickness of 80μm, Wi=1.87, barely exceeding unity. Besides, the reader is reminded that this is the maximum value of Wi over the considered range of SRR, and that in this case, it happens to correspond to the highest considered SRR. As such, most of the corresponding friction curve in that case still falls in the linear regime as evidenced in Figure 4 (right). Therefore, both shear-thinning and limiting-shear-stress mitigate the relative friction increase for T9 (as discussed earlier) to an extent that it becomes higher for PAO4. As the external applied load is increased, the relative friction deviation parameter ξ is reduced for both lubricants by the combination of shear-thinning and limiting-shear-stress effects as evidenced by the increasingly higher values of Wi and Li respectively. This translates into decreasing values of ξ with increased load. Even though limiting-shear-stress and the nonlinear friction regime are slowly reached for PAO4 for loads exceeding 5N, they are penetrated deeper for T9 (as evidenced by the much higher values of Li and Wi) under the same operating conditions resulting in continuously higher ξ values for the former. Note that for the highest loads, namely 25 and 100 N for T9 or also 100N for PAO4, the dominance of limiting-shear-stress brings the relative friction increase to 10% or less whereas for the lower loads where limiting-shear-stress is not reached, values as high as +233.77% are attained. This shows the extent to which limiting-shear-stress dominates the frictional response of a highly loaded EHL contact and overshadows all other effects.

5. Conclusion

This work investigates the effect of lubricant rheology on friction in coated EHL contacts. Two lubricants with relatively different properties are selected: a mineral oil with a relatively high P-T dependence of viscosity and a polyalphaolefin with a relatively low P-T dependence of viscosity. In addition, two coating configurations are considered: the first consists of a soft material with a low thermal inertia while the second is a hard material with a high thermal inertia. The former is known to decrease friction while the latter increases it compared to uncoated contacts. The original expectation was that the lubricant with higher P-T dependence of viscosity would exhibit higher relative friction deviation with respect to the uncoated case than the one with a low P-T viscosity dependence. However, it turned out that this is only true in the linear and thermo-viscous (when reached) friction regimes at relatively low and relatively high SRR respectively. This is because in the former case, contact frictional response is governed by the piezo-viscous behavior of the lubricant while in the latter it is governed by both its piezo-viscous and thermo-viscous responses. In the nonlinear regime, shear-thinning appeared to mitigate friction deviations to an extent that, in some cases, the expectations were contradicted. The same was observed for limiting-shear-stress, which had an even stronger mitigation effect. In fact, when it is reached, lubricant shear stress (which is the governing parameter for friction)

varies only linearly with pressure and very weakly with temperature. In contrast, viscosity variations with pressure which govern frictional response in the linear regime are far stronger than linear. The same applies to viscosity variations with temperature, pressure and shear stress which govern frictional response in the thermo-viscous regime.

Finally, the most relevant conclusion that can be drawn from this work is that EHL friction is, probably and arguably, so complex in nature and involves so many different underlying physics and mechanisms that generic conclusions are difficult to reach.

Nomenclature

η : Lubricant's Generalized Newtonian viscosity
SRR : Slide-to-Roll ratio $= \left(u_b - u_p\right) / u_m$
μ : Lubricant's viscosity
μ_∞ : Lubricant's viscosity extrapolated to infinite temperature
υ_c : Poisson coefficient of coating material
υ_s : Poisson coefficient of substrate material
ρ : Lubricant's density
ρ_R : Lubricant's density at reference state
ρ_c : Density of coating material
ρ_s : Density of substrate material
Λ : Limiting stress-pressure coefficient
τ : Shear stress
τ_L : Limiting shear stress
τ_u : Unbounded shear stress
ξ : Relative friction deviation parameter
c : Lubricant's heat capacity
c_c : Heat capacity of coating material
c_s : Heat capacity of substrate material
C : Lubricant's volumetric heat capacity
f : Friction coefficient
E_c : Young's modulus of elasticity of coating material
E_s : Young's modulus of elasticity of substrate material
F : Contact external applied load
G : Lubricant effective shear modulus
h : Lubricant film thickness
k : Lubricant's thermal conductivity
k_c : Thermal conductivity of coating material
k_s : Thermal conductivity of substrate material
Li : Limiting-shear-stress dimensionless number
p : Pressure
p_h : Hertzian contact pressure

p_0 : Ambient pressure
p_R : Reference pressure
R : Ball's radius
t_c : Coating thickness
T : Temperature
T_0 : Ambient temperature
T_R : Reference temperature
u_b : Ball's surface velocity
u_m : Mean entrainment speed $= \left(u_b + u_p\right)/2$
u_p : Plane's surface velocity
V : Volume
V_R : Volume at reference state
Wi : Weissenberg dimensionless number
x, y, z : Space coordinates

References

[1] Masjedi M. and Khonsari M. - Theoretical and Experimental Investigation of Traction Coefficient in Line-Contact EHL of Rough Surfaces, *Tribology International*, 2014, vol. 70, pp. 179-189.

[2] Xu G. and Sadeghi F. - Thermal EHL Analysis of Circular Contacts with Measured Surface Roughness, *ASME Journal of Tribology*, 1996, vol. 118 (3), doi:10.1115/1.2831560.

[3] Björling M., Larsson R., Marklund P. and Kassfeldt E. - Elastohydrodynamic Lubrication Friction Mapping – The Influence of Lubricant, Roughness, Speed, and Slide-to-Roll Ratio, *IMEchE Part J, Journal of Engineering Tribology*, 2011, vol. 225, pp. 671-681.

[4] Bogdsanski S. – Effect of Coatings on Thermal Conditions of EHL, *Lubrication Science*, 1995, vol. 8 (1), pp. 61-72.

[5] Evans R. D., Cogdell J. D., and Richter G. A. - Traction of Lubricated Rolling Contacts Between Thin-Film Coatings and Steel, *Tribology Transactions*, 2009, vol. 52 (1), pp. 106–113.

[6] Kalin M., Velkavrh I. and Vižintin J. - The Stribeck Curve and Lubrication Design for Non-Fully Wetted Surfaces, *Wear*, 2009, vol. 267 (5-8), pp. 1232–1240.

[7] Björling M., Isaksson P., Marklund P. and Larsson R. – The Influence of DLC Coating on EHL Friction Coefficient, *Tribology Letters*, 2012, vol. 47, pp. 285-294.

[8] Björling M., Habchi W., Bair S., Larsson R. and Marklund P. - Friction Reduction in Elastohydrodynamic Contacts by Thin Layer Thermal Insulation, *Tribology Letters*, 2014, vol. 53, pp. 477-486.

[9] Habchi W., Eyheramendy D., Vergne P. and Morales-Espejel G. – Stabilized Fully-Coupled Finite Elements for Elastohydrodynamic Lubrication Problems, *Advances in Engineering Software*, 2012, vol. 46, pp. 4-18.

[10] Habchi W. – Thermal Analysis of Friction in Coated Elastohydrodynamic Circular Contacts, *Tribology International*, 2016, vol. 93, pp. 530-538.
[11] Bobach L., Bartel D., Beilicke R., Mayer J., Michaelis K., Stahl K., Bachmann S., Schnagl J. and Ziegele H. – Reduction in EHL Friction by a DLC Coating, *Tribology Letters*, 2015, vol. 60 (1), 17.
[12] Bobzin K. and Brögelmann T. – Minimizing Frictional Losses in Crankshaft Bearings of Automobile Powertrain by Diamond-Like Carbon Coatings under Elastohydrodynamic Lubrication, *Surface and Coatings Technology*, 2016, vol. 290, pp. 100-109.
[13] Beilicke R., Bobach L. and Bartel D. – Transient Thermal Elastohydrodynamic Simulation of a DLC Coated Helical Gear Pair Considering Limiting Shear Stress Behavior of the Lubricant, *Tribology International*, 2016, vol. 97, pp. 136-150.
[14] Habchi W. - Influence of Thermo-Mechanical Properties of Coatings on Friction in Elastohydrodynamic Lubricated Contacts, *Tribology International*, 2015, vol. 90, pp. 113-122.
[15] Björling M., Larsson R. and Marklund P. - The Effect of DLC Coating Thickness on Elastohydrodynamic Friction, *Tribology Letters*, 2014, vol. 55, pp.353-362.
[16] Murnaghan F. D. - The Compressibility of Media under Extreme Pressures, *Proceedings of the National Academy of Sciences*, 1944, vol. 30, p. 244-247.
[17] Roland C. M., Bair S. and Casalini R. - Thermodynamic Scaling of the Viscosity of Van Der Waals, H-bonded, and Ionic Liquids, *Journal of Chemical Physics*, 2006, vol. 125 (12), 4508.
[18] Bair S. and Casalini R. - A Scaling Parameter and Function for the Accurate Correlation of Viscosity with Temperature and Pressure Across Eight Orders of Magnitude of Viscosity, *Journal of Tribology*, 2008, vol. 130 (4), 041802.
[19] Habchi W., Vergne P., Bair S., Andersson O., Eyheramendy D. and Morales-Espejel G. E. – Influence of Pressure and Temperature Dependence of Thermal Properties of a Lubricant on the Behaviour of Circular TEHD Contacts, *Tribology International*, 2010, vol. 43, pp. 1842-1850.
[20] Bair S. and Qureshi F. - Accurate Measurements of Pressure-Viscosity Behavior in Lubricants, *STLE Tribology Transactions*, 2002, vol. 45 (3), pp. 390 – 396.
[21] Bair S. - The High Pressure Rheology of Some Simple Model Hydrocarbons, *IMechE Part J, Journal of Engineering Tribology*, 2002, vol. 216, pp. 139 - 149.
[22] Bair S. - A Rough Shear Thinning Correction for EHD Film Thickness, *STLE Tribology Trans.*, 2004, vol. 47, pp. 361-365.
[23] Liu P., Yu H., Ren N., Lockwood F. E. and Wang, Q. J. - Pressure–Viscosity Coefficient of Hydrocarbon Base Oil through Molecular Dynamics Simulations, *Tribology Letters*, 2015, vol. 60(3), pp. 1-9.
[24] Bair S. and Winer, W. O. - The high shear stress rheology of liquid lubricants at pressures of 2 to 200 MPa, *ASME Journal of Tribology*, 1990, vol. 112(2), pp. 246-252.

[25] Nagata Y. – EHD Phenomena in Grease Lubricated Contacts, *PhD Thesis*, University of Sussex, UK, 2011.
[26] Habchi W., Bair S. and Vergne P. – On Friction Regimes in Quantitative Elastohydrodynamics, *Tribology International*, 2013, vol. 58, pp. 107-117.
[27] Bair S., Vergne P., Kumar P., Poll G., Krupka I., Hartl M., Habchi W. and Larsson R. - Comment on "History, Origins and Prediction of Elastohydrodynamic Friction" by Spikes and Jie, *Tribology Letters*, 2015, *58*:16, doi:10.1007/s11249-015-0481-x.
[28] Habchi W. – A Numerical Model for the Solution of Thermal Elastohydrodynamic Lubrication in Coated Circular Contacts, *Tribology International*, 2014, vol. 73, pp. 57-68.
[29] Bird R. B., Armstrong R. C. and Hassager O. - Dynamics of Polymeric Liquids, Vol.: 1 Fluid Mechanics, second edition, *Wiley*, New York, 1987, p 94.
[30] Bair, S. and Kotzalas, M., "The Contribution of Roller Compliance to Elastohydrodynamic Traction", STLE *Tribology Trans*., Vol.49, No.2, 2006, pp. 218-224.
[31] Bair, S.: High-Pressure Rheology for Quantitative Elastohydrodynamics, Elsevier Science, Amsterdam (2007), pp. 173-174.